Insight into the Intraparticle Diffusion of Residue Oil Components in Catalysts During Hydrodesulfurization Reaction

Zhigang Wang, Sheng-Li Chen, Jianing Pei, Aicheng Chen, Junhui Zhang, and Zhiming Xu
State Key Laboratory of Heavy Oil Processing, Chemical Engineering Dept., College of Chemical Engineering, China University of Petroleum, Beijing 102249, P.R. China

Jay B. Benziger
Dept. Chemical and Biological Engineering, Princeton University, Princeton, NJ 08544

DOI 10.1002/aic.14501
Published online June 2, 2014 in Wiley Online Library (wileyonlinelibrary.com)

Well-defined and uniform pore structure catalysts were used to study the intraparticle diffusion of fractionated Saudi vacuum residue under hydrodesulfurization (HDS) reaction conditions. HDS rates of residue oil cuts with different molecular weights are determined as functions of pore size, temperature, and pressure in a trickle-bed reactor. Credible intrinsic and bulk diffusivities of organosulfur compounds in residue oil were obtained for the first time, from the apparent and intrinsic reaction kinetic constants. Intrinsic diffusivities ranged from 2×10^{-7} *to* 8×10^{-7} cm^2/s *for the residual oil molecules; diffusivity decreases with increasing molecular weight of the residual oil. The intrinsic diffusivity for molecular weights ~1000 Daltons increases with pore size for pores <70 nm, but is nearly independent of pore size for pores >70 nm. The diffusivity dependences on pore size and molecular weight suggest that the onset of restricted diffusion occurs for ratios of molecular diameter to pore diameter of ~0.04.* © 2014 American Institute of Chemical Engineers *AIChE J*, 60: 3267–3275, 2014
Keywords: diffusion, pore-size distribution, hydrodesulfurization

Introduction

Increased production of high sulfur containing heavy crude oil coupled with increasing demand for petroleum products with reduced sulfur content, has elevated the importance of hydrodesulfurization (HDS) to remove sulfur.[1] Due to the low vapor pressure of residue oil molecules HDS is most often performed in a three-phase trickle-bed reactor. The intraparticle diffusion rate of organosulfur compounds in residue oils inside catalyst is low. Consequently, the HDS overall reaction rate is often limited by intraparticle diffusion, resulting in limited catalyst utilization. Reactant molecules diffusion into the catalyst particle is limited during the reactor residence time.[2–4] Characterization of intraparticle diffusion of residue oil molecules within catalyst pores under HDS reaction conditions can assist in the design of efficient catalysts.

The diffusion of reactants in porous materials depends on pore size and pore structure.[5] Diffusion is severely restricted when a reactant molecule is about the same size of a catalyst pore. This phenomenon is referred to as restrictive or configurational diffusion.[6] Restrictive diffusion is well known in zeolites, where the ratio of the pore size to the molecular diameter is ~1. But little is known about the onset of restricted diffusion; at what ratio of molecular size to pore size does diffusion deviate from bulk diffusion?

Correspondence concerning this article should be addressed to S.-L. Chen at slchen@cup.edu.cn.

Many researchers have investigated diffusion of residue oil in catalyst pores by diaphragm,[7–10] sorptive,[11–13] and reaction-kinetic methods.[14–18] Our research group has developed a method of preparing catalyst supports with well-defined pore structures. We measured the effective diffusivities of extracted oil fractions in a uniform pore-size SiO_2 by the sorptive method at room temperature. We have recently extended our methodology to deposit active catalytic materials on the surfaces of SiO_2 opals. This process results in well-defined uniform-pore structure (WDUPS) catalysts. Catalysts are based on well-defined packing of uniform spheres, resulting in catalysts that have identical porosity and tortuosity independent of pore size; and we used this WDUPS catalysts to measure the intraparticle diffusion of nickel-porphyrin under hydrodemetallization reaction conditions.[19] In this article, we report the preparation of well-defined uniform-pore HDS catalysts. The effective and intrinsic diffusivities of reactive organosulfur compounds in these catalysts have been measured under reaction conditions.

At steady state, HDS catalysis requires countercurrent diffusion of species in the catalyst pores. Organosulfur molecules and H_2 are transported from the external surface of the catalyst particles to the active reaction sites along the walls of the catalyst pores. Desulfurized molecules and H_2S are transported from the active sites in the catalyst pores to the external surface of the catalyst particles. The effective diffusivity involves contributions from diffusion of all those species.

Reaction-kinetic methods have been used with conventional HDS catalysts. However, the conventional CoMo/

Al_2O_3 HDS catalyst has a broad pore-size distribution. The variable pore-size distribution and pore connectivity makes it difficult to distinguish intrinsic catalytic kinetics from reactant transport.[20] For instance, Philippopoulos and Papayannakos[21] investigated the intraparticle diffusion of residue oil over two types of commercial $CoMo/A1_2O_3$ catalysts in a trickle-bed reactor. Their results showed that the effective diffusion coefficient of residue oil in the catalyst with broad pore-size distribution was approximately three times larger than that in the catalyst with the same average diameter but unimodal pore-size distribution. Because the tortuosity factor of the conventional catalysts is unknown (or vague), one can only obtain the effective diffusivity. Because the porosity and tortuosity of the WDUPS catalyst are well defined, we can more clearly distinguish kinetic and transport contributions.

A second complication associated with measuring HDS kinetics is the variability of diffusion coefficients and rate constants associated with complex industrial feedstocks.[15,17,22] Given the extreme difference between the single-structured model compounds and the complex molecules in residue oil, the diffusivity of model compounds may not agree with that of residue molecules under industrial HDS conditions. Fractionated cuts of industrial feedstocks obtained by supercritical fluid extraction and fractionation (SFEF) technique can provide samples that retain the molecular structure of the industrial feedstock.[23] These fractionated cuts have a narrow distribution of molecular sizes, which should provide a narrow range of diffusivities. We suggest that these residual oil cuts are more appropriate model samples for investigation of intraparticle diffusion of HDS. To our best knowledge, studies about intraparticle diffusion of residue oil molecules of different narrow cuts within WDUPS catalyst under HDS reaction conditions have not been reported yet.

The aim of this article is to investigate the intraparticle diffusion of residue oil molecules in five $NiMo/Al_2O_3$-SiO_2 WDUPS catalysts with the same porosity and tortuosity. By systematic variation of catalyst particle size and pore size, we obtain the intrinsic diffusivity as functions of molecular size, reaction temperature, pressure, and H_2/Oil ratio (v/v). Based on intrinsic diffusivity of different molecular weight cuts of residue oil, it is possible to identify the ratio of molecular size to pore size for the onset of restricted diffusion.

Experimental

Feedstock

SFEF was used to separate Saudi vacuum residue oil into 15 narrow extractable fractions and a nonextractable end-cut. The details and operation procedure of the SFEF process have been described elsewhere.[24–26] Sulfur-free Lube base oil, supplied by Sinopec Shanghai Gaoqiao Petrochemical Corporation (China), was used as solvent; it was a good solvent for SFEF fractions of residue oil and had a negligible cracking rate at the HDS reaction conditions. The residue oil fraction in the solutions is 4 wt %. Five narrow residue oil fractions were used in experiment, and the prosperities are summarized in Table 1.

The sulfur content in the narrow residue oil fractions was measured by a THA-2000S UV-induced fluorescence sulfur analyzer (Taizhou Jinhang Analytical Instruments Co., China). The molecular weight distribution of narrow fractions of residue oil was measured by gel permeation chromatography (P230HLPC at 35°C; Elite Co., China), with tetrahydrofuran as solvent. The equivalent spherical diameter of molecules of the SFEF cuts was estimated from Eq. 1 suggested by Chung et al.[27]

Table 1. Properties of SEFE Narrow Fraction Cuts of Saudi Vacuum Residue

Sample	Molecular Weight	Average Diameter (nm)	Sulfur (wt%)
Sa-1#	786	1.54	3.21
Sa-5#	1010	1.77	3.45
Sa-7#	1080	1.83	3.51
Sa-11#	1160	1.90	3.55
Sa-14#	1280	2.00	5.14

$$d_m = 0.0403\ M_w^{0.537} \quad (1)$$

where d_m is the equivalent spherical diameter (nm) of molecules of an SFEF cut and M_w is the molecular weight of an SFEF cut.

Catalysts

The WDUPS catalysts were prepared by first preparing the opal SiO_2 materials, then coating Al_2O_3 on to the surface of the opal SiO_2 materials to switch the SiO_2 surface to Al_2O_3 surface which is needed as the HDS catalyst supports, and finally supporting the HDS catalytically active components on to the Al_2O_3-modified SiO_2 opals.[28–30] The opal SiO_2 materials were prepared by self-assembly of monodisperse silica spheres, which were prepared through hydrolysis and condensation of tetraethyl orthosilicate in alcohol and in the presence of water and ammonia. In a typical SiO_2 opal assembly process, a suspension of SiO_2 microspheres was put into a glass beaker. The beaker was then placed into an oven and kept at 50°C with a relative humidity of 90%. After several days, the SiO_2 microspheres were automatically assembled into faced-center cubic lattices (i.e., the close packing of spheres, also called opal structure) when the suspension was dried. During the assembling process of the SiO_2 microspheres, two forces, that is, the repulsive force created by the Zeta potential of the colloidal SiO_2 microspheres and the gravity force, are applied on the SiO_2 microspheres and these two forces are balanced. There are two potential energies involved in the SiO_2 microspheres suspension—the Zeta potential energy and the gravity potential energy. It is the minimization of the total potential energies that assembles the SiO_2 microspheres in to the opal structure. The as-prepared SiO_2 opal was calcined in muffle furnace at 700°C for 2 h to strengthen the SiO_2 opal. The prepared SiO_2 opal was impregnated with the $Al(NO_3)_3$ solution by the incipient-wetness impregnation method, followed by hydrolysis in ammonia/water vapor for 6 h and an additional dry at 100°C for 12 h. Thus, an Al_2O_3 layer was deposited on the SiO_2 opal with the loading of 4.5 μmol $(Al_2O_3)/m^2$-SiO_2 after calcination at 500°C for 5 h.

The Al_2O_3-SiO_2 supports were coimpregnated with a solution of nickel nitrate, ammonium molybdate, and EDTA to prepare $NiMo/Al_2O_3$-SiO_2 WDUPS catalyst with loadings of 5.42 μmol (Mo)/m^2-support and 1.75 μmol (Ni)/m^2-support. An EDTA to Ni molar ratio of 2 and a pH of 9 was

Table 2. Characteristics of $NiMo/Al_2O_3$-SiO_2 WDUPS Catalysts

Catalysts	BET Surface Area (m^2/g)	Average Pore Diameter (nm)	Pore Volume (cm^3/g)	Porosity	Particle Density (g/cm^3)	Tortousity Factor
AR-50	46.94	15.3	0.18	0.28	1.58	1.52
AR-100	31.97	27.5	0.22	0.33	1.48	1.46
AR-200	19.88	48.3	0.24	0.35	1.44	1.44
AR-300	15.43	70.0	0.27	0.37	1.38	1.40
AR-500	7.45	102.0	0.22	0.33	1.41	1.45

maintained during the coimpregnation process. The $NiMo/Al_2O_3$-SiO_2 WDUPS catalyst particles were dried in air at room temperature for 12 h, then at 120°C for 12 h. Five different pore-sized NiMo-EDTA/Al_2O_3-SiO_2 WDUPS catalysts were prepared, denoted as AR-50, AR-100, AR-200, AR-300, and AR-500 where the number denotes the diameter of silica spheres in nm used to make the base silica opal serving as the catalyst support.

The brunauer -emmett -teller (BET) surface area of the NiMo-EDTA/Al_2O_3-SiO_2 WDUPS catalysts were determined by nitrogen adsorption at −196.15°C using a Micromeritics ASAP 2010 surface area analyzer (Micromeritics). The pore-size distribution of the catalyst was measured by the mercury penetration method on an auto pore IV9500 mercury porosimeter (Micromeritics) assuming a contact angle of 140°. The catalysts' characteristics are listed in Table 2; the pore-size distribution is shown in Figure 1. The tortuosity of the $NiMo/Al_2O_3$-SiO_2 WDUPS catalyst is estimated from the following empirical equation

$$\tau = 1 + 0.41 \ln(1/\varepsilon) \quad (2)$$

where τ is the tortuosity factor of catalyst, ε is the porosity of catalyst. Eq. 2 was derived from the porous materials made by compact packing of nonporous microspheres,[31] and should provide good estimates of the WDUPS catalysts tortuosity factors.

The average pore diameter of the five catalysts ranged from 15.3 to 102 nm. The narrow pore-size distributions shown in Figure 1 are indicative of packing of uniform particles. Because all the model catalysts were made from uniform SiO_2 spheres they had nearly identical fractional pore volume, and pore tortuosity. The average pore volume is 0.33 cm^3/g and the average pore tortuosity is 1.46.

The morphology of AR-300 WDUPS catalyst with a FEI quanta 200F SEM (FEI) is shown in Figure 2. The AR-300 catalyst was an opal-like material with face-centered cubic packing of monodisperse nonporous spheres.

Experimental procedures

HDS of residue oil fractions was performed in a stainless-steel trickle-bed reactor with 9-mm internal diameter and 500-mm length. WDUPS catalysts were crushed and sieved. Five fractions with mean equivalent diameters of 0.128, 0.25, 0.38, and 0.675 mm were recovered for testing. The catalyst size distribution was measured by the CX21 optical microscope (Olympus Corporation, Japan) equipped with PTP 8.1 particle image processor (Zhuhai OMEC Instrument Co., China). The magnification of the optical microscope was calibrated with a National Institute of Standard and Technology stage micrometer (SRM 2800), and the measured catalyst size distribution is shown in Figure 3. It could be found that the size distribution of relative large catalyst pellets approached to uniform distribution, whereas the small catalyst pellets tended to distribute in normal distribution. A variety of methods have been proposed to reduce nonuniformities of gas and liquid flow through the trickle-bed reactor.[32–35] We diluted the catalyst with chemically inert quartz sand to improve flow uniformity. The reactor was loaded with catalyst to a height of 45 mm.

The catalyst was sulfided by pumping a mixture of 2 wt % CS_2 and cyclohexane into the reactor. The reactor temperature was raised from room temperature to 230°C at 7°C/min and held at 230°C for 3 h. The temperature was then raised to 340°C at 3°C/min and held for 3 h.

After sulfidation, the feed was switched to the HDS feedstock and maintained for 20 h to achieve catalyst stability. The reaction conditions were as follows: surface hourly space velocity (SHSV), 1–7 × 10^{-6} m/h; H_2/Oil ratio (the ratio of H_2 gas volume under the standard state (273.15 K and 1 atm) to the liquid oil volume at room temperature), 400–1000; pressure, 4.0–10.0 MPa; temperature, 355–400°C.

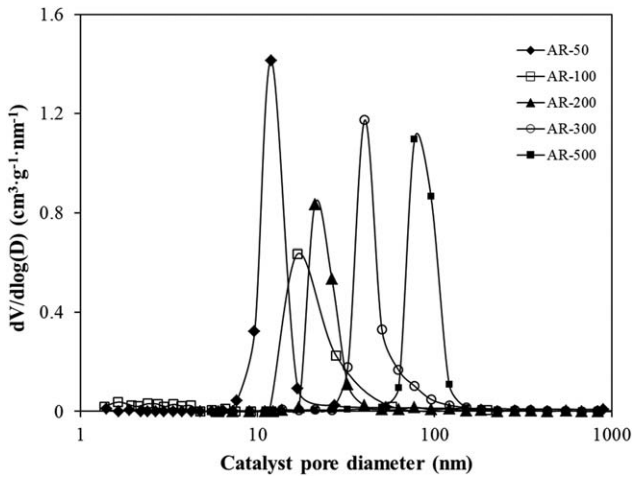

Figure 1. Pore diameter distribution of five $NiMo/Al_2O_3$-SiO_2 WDUPS catalysts.

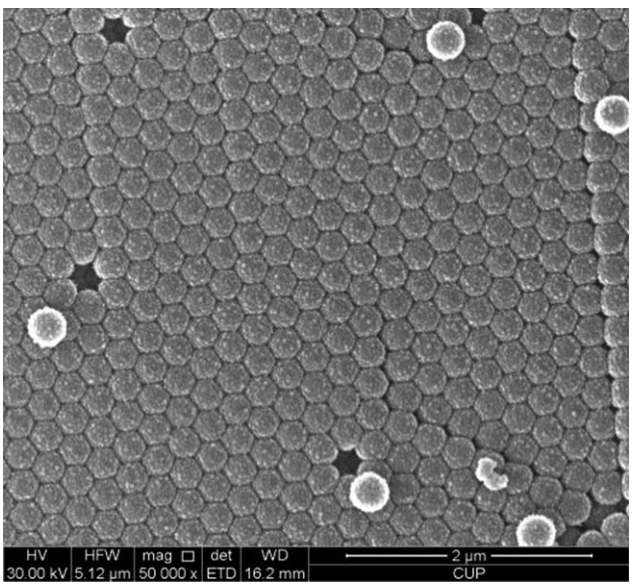

Figure 2. SEM image of AR-300 WDUPS catalyst.

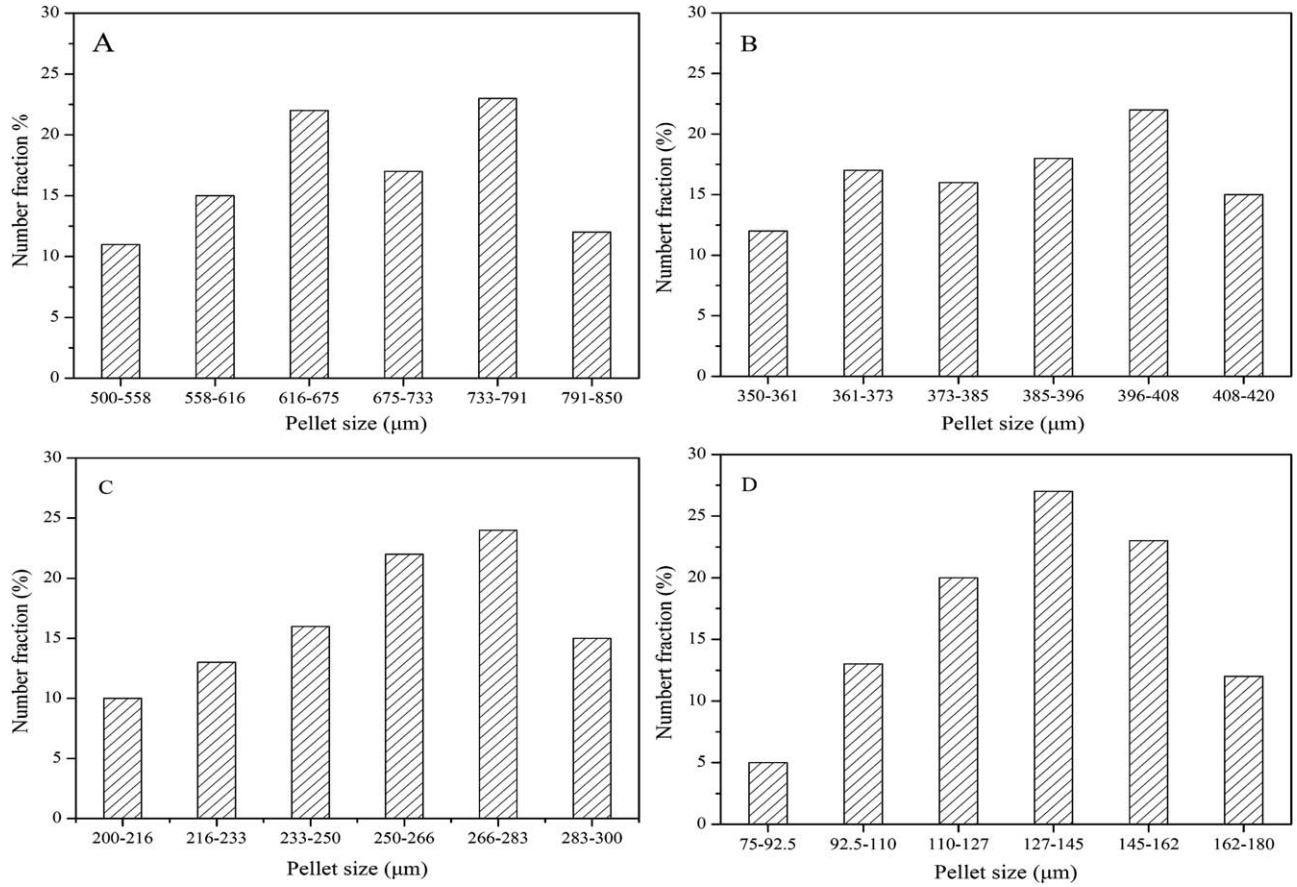

Figure 3. Particle-size distribution of catalysts with mean equivalent diameters of 0.675 mm (A), 0.38 mm (B), 0.25 mm (C), and 0.128 mm (D).

Product samples were periodically collected and washed three times with a 5 wt % sodium hydroxide solution to remove H_2S dissolved in the samples. The sulfur content in the samples was measured by a THA-2000S UV-induced fluorescence sulfur analyzer (Taizhou Jinhang Analytical Instruments Co., China).

Removal of internal diffusion resistance for the measurement of intrinsic kinetic data

HDS reactions of 4 wt % Sa-1# and Sa-14# solutions over AR-50 catalyst of different particle sizes were performed at 400°C, 6.0 MPa, H_2/Oil (v/v) = 800, SHSV = 2.12×10^{-6} m/h. In this work, SHSV is applied to describe the ratio of liquid feedstock flow rate to catalyst surface area (m^3-oil h^{-1}/m^2-cat.). As shown in Figure 4, the HDS rate per catalyst surface area increased as the catalyst particle size decreased from 0.675 to 0.25 mm, and then remained nearly constant with further decrease of catalyst particle size. These results indicated that the internal diffusion resistance is negligible when the catalyst particle size was <0.25 mm, but at larger catalyst particle size, there is a measurable diffusional resistance. Throughout the rest of this study, we assume that diffusional resistances can be neglected for catalyst particle size <0.25 mm, so that intrinsic kinetic data were measured over a catalyst with 0.128-mm particle size. The apparent (diffusion limited) kinetic data were measured over a catalyst with 0.675-mm particle size, and the diffusivities were obtained through the difference between the diffusion limited kinetic data and the intrinsic kinetic data.

Data Treatment

HDS was performed in an isothermal and plug-flow reactor; the differential material balance of the reactor is given by Eq. 3

$$-\frac{dC}{dS} = \frac{\eta k_n C^n}{Q} \tag{3}$$

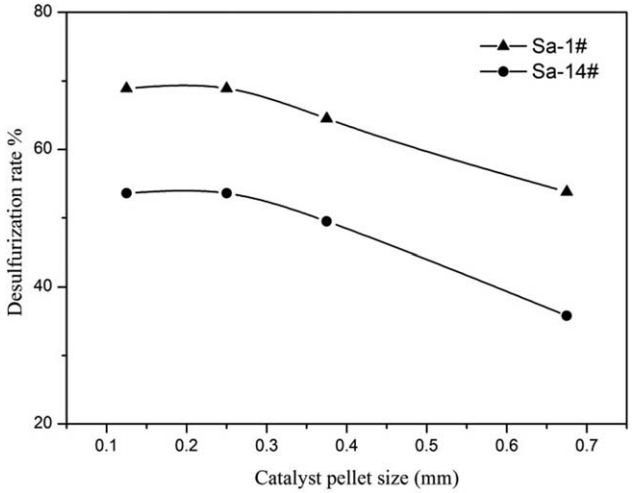

Figure 4. Relationship between HDS rate and catalysts pellet size (AR-50 catalyst, 400°C, 6.0 MPa, H_2/Oil ratio (v/v) = 800, SHSV = 2.12×10^{-6} m/h).

where C is the concentration of the reactant (g/m^3) in bulk phase; S is the surface area of the catalyst loaded in the reactor (m^2); k_n is the intrinsic rate constant with a unit depended on the reaction order n; η is the catalyst effectiveness factor; Q is the feedstock flow rate (m^3/h). Eq. 3 assumes that the hydrogen concentration is constant, so the reaction rate only dependents on the organosulfur concentration. Previous researchers[22,36] have recognized that HDS reactions of an individual compound follow first-order kinetics.

For $n = 1$, Eq. 3 can be integrated as

$$\ln \frac{C_0}{C_t} = \frac{\eta k_i}{\mathrm{SHSV}} = \frac{k_a}{\mathrm{SHSV}} \tag{4}$$

$$\mathrm{SHSV} = \frac{Q}{S} \tag{5}$$

where C_0 and C_t are the sulfur concentration in the feedstock and product stream, respectively (g/m^3), k_i and k_a are the intrinsic and apparent kinetic pseudo-first-order reaction rate constant, respectively (m/h).

The crushed catalysts were regarded as spherical pellets, with effectiveness factor, η, given by Eq. 6

$$\eta = \frac{k_a}{k_i} = \frac{3}{\phi}\left(\frac{1}{\tanh \phi} - \frac{1}{\phi}\right) \tag{6}$$

where ϕ is the Thiele modulus which is defined by Eq. 7

$$\phi = R\left(\frac{k_i \rho_c S_g}{D_e}\right)^{0.5} \tag{7}$$

where D_e is the effective diffusivity of reactant molecules in the catalyst (m^2/h); R is the radius of the catalyst particle (m); ρ_c is the particle density of catalyst (g/m^3); S_g is the specific surface area of the catalyst (g/m^2)

Eq. 7 can be rearranged to express the effective diffusivity, D_e, in terms of experimentally determined quantities, as shown in Eq. 8

$$D_e = \frac{R^2 k_i \rho_c S_g}{\phi^2} \tag{8}$$

The rate constants k_a and k_i were determined by from the slope of $\ln(C_0/C_t)$ and SHSV^{-1}; k_i was obtained for 0.125-mm catalyst particles (where it is assumed $\eta = 1$) and k_a was obtained for the 0.675-mm catalyst particles. η and ϕ were determined by Eq. 6 from the values of k_i and k_a; and finally D_e was calculated by Eq. 8.

Beck and Shultz proposed Eq. 10 to estimate the diffusion coefficient in a porous media. They assume diffusion is inhibited by the size of the pore[37]

$$D_e = \frac{D_b \varepsilon}{\tau} F(\lambda) \tag{9}$$

where

$$F(\lambda) = (1-\lambda)^z \tag{10}$$

$$\lambda = \frac{d_m}{d_p} \tag{11}$$

D_b is the bulk diffusivity; λ is the ratio of reactant molecule size to catalyst pore size; $F(\lambda)$ is the restrictive factor; where z indicates the magnitude of restrictive effect; that is, the larger value of z, the more significant the restrictive effect at a given λ. A plot of $\ln D_e$ vs. $\ln(1 - \lambda)$ will yield a straight line with a slope of z. Eq. 9 indicates diffusion can be restricted even when the molecular diameter is a fraction of the pore diameter. There is an effective drag on molecular diffusion which depends on the average distance from the molecule to the pore wall.

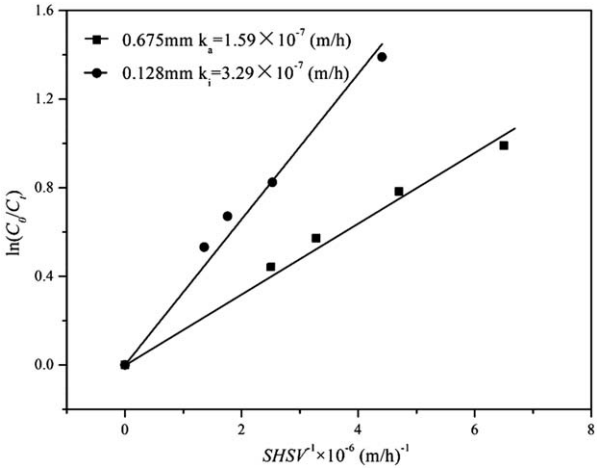

Figure 5. Relationship between $\ln(C_0/C_t)$ and SHSV^{-1} for Sa-14# narrow cut over catalyst with particle sizes of 0.128 and 0.675 mm, respectively.

The intrinsic diffusivity (D_i) is the diffusivity in pores and is defined as follows

$$D_i = D_b F(\lambda) \tag{12}$$

D_i is the local diffusivity in a single pore. It is independent of τ and ε, and equal to the D_b when the pore size is large enough ($F(\lambda \rightarrow 0) = 1$). The effective diffusivity, D_e, depends not only on the bulk diffusivity and the pore size, but on the tortuosity and porosity of the catalyst. The intrinsic and effective diffusivities are related by Eq. 13

$$D_i = D_e \frac{\tau}{\varepsilon} \tag{13}$$

The WDUPS catalysts with different particle sizes are geometrically identical and thus, have definite τ and ε, independent of pore size. Thus, we can obtain D_i through D_e, τ, and ε of the WDUPS catalysts.

Sample data of $\ln(C_0/C_t)$ and SHSV^{-1} obtained using 4 wt % Sa-14# solution as feedstock at different reaction SHSVs, is shown in Figure 5. The best fit straight lines of $\ln(C_0/C_t)$ vs. SHSV^{-1} are consistent with the assumption that the HDS reactions of Sa-14# narrow fraction are pseudo-first-order manner, and the slopes of the two straight lines were the intrinsic and apparent reaction rate constants, respectively. The reaction order for HDS of the other solutions (Sa-1#, Sa-5#, Sa-7#, Sa = 11#) was also found to be first order.

Results and Discussion

Catalyst pore diameter

To investigate the effect of catalyst average pore size on diffusivity of residue oil molecules under reaction conditions, HDS reactions of Sa-1#, Sa-7#, and Sa-14# residue oil cuts were preformed over five WDUPS catalysts with average pore sizes from 15.3 to 102 nm. Reactions were performed with catalyst particle sizes of 0.128 and 0.675 mm.

Table 3. The $D_e \times 10^7$ cm^2/s and $D_i \times 10^7$ cm^2/s of Residue Oil Cut Under Different Pore Size (400°C, 6.0 MPa, H_2/Oil ratio (v/v) = 800)

Catalysts	Average Pore Diameter (nm)	$D_e \times 10^7$ (cm^2/s)			$D_i \times 10^7$ (cm^2/s)		
		Sa-1#	Sa-7#	Sa-14#	Sa-1#	Sa-7#	Sa-14#
AR-50	15.3	1.36	0.897	0.392	6.02	3.97	1.73
AR-100	27.5	1.43	1.09	0.547	6.33	4.82	2.42
AR-200	48.3	1.70	1.24	0.667	7.52	5.49	2.95
AR-300	70.0	1.72	1.33	0.710	7.61	5.88	3.14
AR-500	102.0	–	–	0.702	–	–	3.11

The reaction conditions were as follows: 400°C, 6.0 MPa, H_2/Oil ratio (v/v) = 800.

As shown in Table 3, intrinsic diffusivity (D_i) was in the range of $2 \times 10^{-7} - 8 \times 10^{-7}$ cm^2/s for the three sulfur-containing fractions of residue oil in WDUPS catalysts. The tortuosity, which is unknown (or vague) for conventional catalysts and definite for the WDUPS catalysts, is indispensable to the intrinsic diffusivity. It is the first time for people to obtain the creditable intrinsic diffusivity at the HDS conditions of petroleum residua. D_i and D_e of reactant molecules, in catalysts with the same pore size increased with decreasing molecular weight of the residue oil fraction. This suggests that catalyst effectiveness may be misinterpreted if the diffusivity of residue oil molecules of different molecular weight is approximated by using one average effective diffusivity.[15]

The molecular weights of the oil cuts have a greater impact on intrinsic diffusivity than the catalyst pore diameter. The diffusivities change much more across a row in Table 3 (corresponding to increasing molecular weight) than going down a column (corresponding to increasing pore diameter). The diffusivities show the most significant decrease with pore size for the highest molecular weight.

The effective and intrinsic diffusivity of Sa-14# were almost constant for AR-200, AR-300, and AR-500, suggesting the internal diffusion was almost free diffusion. This was also true for the Sa-1# and Sa-7# Therefore, the D_b for Sa-1#, Sa-7#, and Sa-14# is about 7.61×10^{-7}, 5.88×10^{-7}, and 3.14×10^{-7} cm^2/s. Because we used the WDUPS catalysts as the experimental materials, we were able to obtain the bulk diffusivity at the HDS reaction conditions through internal diffusion study.

The effective diffusivity increased with increased pore diameter for the Sa-14# sample from the AR-50 to AR-200 catalyst, suggesting the internal diffusion is limited to a certain extent by the pore size of the catalyst. This suggests that the onset for restricted diffusion is $\lambda - 0.04$ (2.0/48). The restrictive factor, $F(\lambda)$, was calculated according to Eq. 12 and the results are shown in Figure 6. For comparison, the $F(\lambda)$ data from literatures are also shown in Figure 6. It can be seen that the $F(\lambda)$ from our experimental data agree well with those reported in literatures.

The exponent, z, in the Beck and Shultz[37] model is a measure of the restricted diffusion. A plot of $\ln D_e$ vs. $\ln(1 - \lambda)$ yields a straight line with a slope of z, the magnitude of restrictive effect. As shown in Figure 5, the values of z for Sa-1#, Sa-7#, and Sa-14# were 2.0, 2.66, and 3.22, respectively. Obviously, the restrictive diffusion increases with molecular weight.

In previous studies,[14–16,18] the Stokes–Einstein and Wilke–Chang equations[39] were used to estimate the bulk diffusivity. However, these equations are only applicable when solution concentration is low and there are no wall effects. Estimates from these equations do not consider the countercurrent diffusion of the reactants and products occurring at steady state. Measuring the effective diffusivities in WDUPS catalyst is a viable way to obtain bulk diffusivity under reactive conditions.

Reaction temperature

The effect of temperature on the intrinsic diffusivity of residue oil molecules was probed with the AR-200 and AR-50 catalysts. The reaction conditions were as follows: 355–400°C, 6.0 MPa, H_2/Oil ratio = 800.

As shown in Figure 7, the intrinsic diffusivity of the three narrow fractions of residue oil increased approximately linearly with reaction temperature. The increase is expected. It reflects increased kinetic energy of the solute and reduced solvent viscosity at higher temperature. The effect of temperature on the diffusivity was studied by several researchers. Lee et al.[40] and Galiasso and Morales[41] reported that the effective diffusivity increased with reaction temperature, and found that the effective diffusivity increased more rapidly than calculated bulk diffusivity does with temperature. They suggested that the hydrodynamic drag and effective pore size affected by adsorption capacity of solute and solvent may be different at different temperature. At higher temperature, the adsorption capacity declined, the hydrodynamic drag decreased, and the effective pore size increased, therefore, effective diffusivity increased more rapidly than calculated bulk diffusivity. However, the pore size of catalyst we used

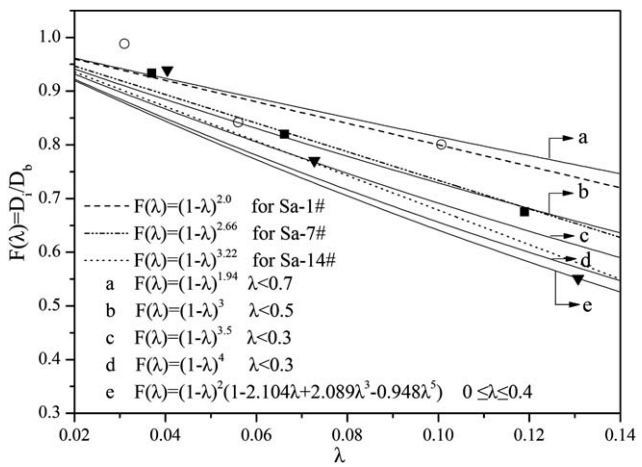

Figure 6. Comparison of experimental restrictive factor data with literature correlations [a and b: Ref. 16, c: Ref. 17, d: Ref. 37, and e: Ref. 38).

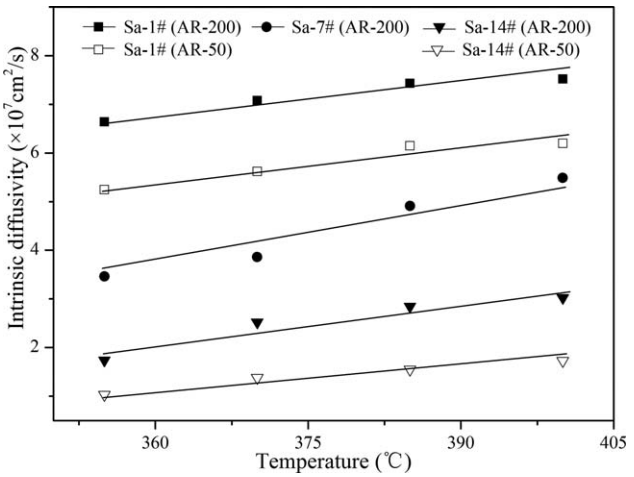

Figure 7. Effect of temperature on intrinsic diffusivity (6.0 MPa, H_2/Oil ratio (v/v) = 800).

(about 48 nm) was much more larger than that of they used (ranged from 6.2 to 19.8 nm), the change in the pore size caused by adsorption capacity was not significant. Seo and Massoth[42] also investigated the effect of temperature on the effective diffusivity of three model molecules by sorptive methods, and calculated the bulk diffusivity of them by Stokes–Einstein equation. He suggested that diffusing molecules had a large kinetic energy at elevated temperature, so the molecules could more easily pass through an energy barrier resulting from hydrodynamic drag. Additionally, his experimental data showed the bulk diffusivity of solute increased approximately linear relationship with temperature, whereas the effective diffusivity did not. According to the Stokes–Einstein equation, the bulk diffusivity changes approximately linearly with the temperature in a certain temperature range. The intrinsic diffusivity without significant restricted effect is close to bulk diffusivity, so that this linear relationship was observed. The effect of molecular weight and pore size on diffusivity is greater than the effect of temperature. It is evident in Figure 6 that the difference of D_i of Sa-1 and Sa-14 on AR-50 between 350and 400°C is less than the difference of D_i between Sa-1 and Sa-14 on AR-50 or the difference of D_i of Sa-1 between AR-50 and AR-200.

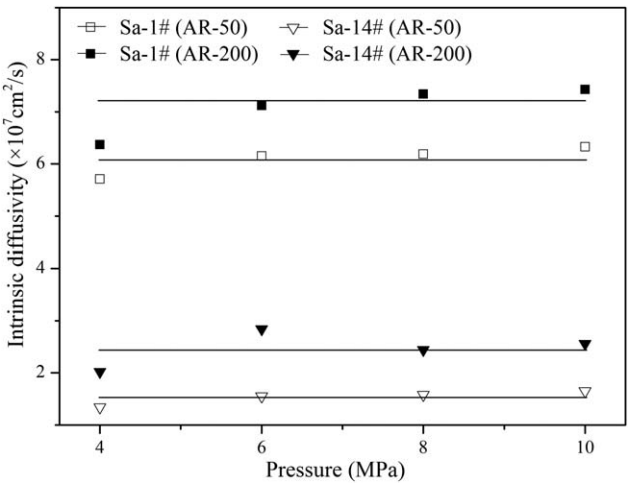

Figure 8. Effect of hydrogen pressure on intrinsic diffusivity of residual oil fractions (385°C, H_2/Oil ratio (v/v) = 800).

Pressure

The effect of hydrogen pressure on the intrinsic diffusivity of residual oil molecules within the catalyst pores under HDS conditions was studied in the range of 4.0 – 10.0 MPa on AR-200 and AR-50 catalysts. The reaction conditions were as follows: 385°C, H_2/Oil ratio = 800.

Seo and Massoth[42] reported that hydrogen pressure had no effect on the intrinsic diffusivity of molecule. However, Wang et al.[14] found that effective diffusivity of residue oil molecules increased with increasing hydrogen pressure, and attributed the phenomenon to the variation of hydrogen solubility in diesel under different hydrogen pressures. Our experimental result, as shown in Figure 8, indicates that intrinsic diffusivity of residual oil fractions with different pore-size catalysts was almost independent of the hydrogen pressure, in agreement with the results of Massoth. According to Cai et al.[43] and Prather et al.[44] reports, the hydrogen solubility in heavy oil or recycle oil was about 0.5–1 g per 1 Kg oil under 380°C in the range of 4.0–10.0 MPa, indicating that the hydrogen solubility in heavy oil of was very low. Therefore, the effect of solubility change caused by the hydrogen pressure on effective diffusivity is negligible. In addition, because liquid viscosity increases with pressure slightly,[45] and the pressure-variation range of our experiment was not so much wide, the effect of pressure on the viscosity was very small. Therefore, the hydrogen pressure had not noticeable impact on intrinsic diffusivity.

H_2/Oil ratio

The effect of H_2/Oil ratio on the intrinsic diffusivity of residue oil molecules within the WDUPS catalyst under HDS condition was studied in the range of 400–1000. The reaction conditions were as follows: AR-200 catalyst, 400°C, 6.0 MPa; 4 wt % Sa-5# and Sa-11# solutions were used as feedstock in this experiment.

As shown in Figure 9, the intrinsic diffusivity of residue oil molecules does not change with H_2/Oil ratio, indicating that the H_2/Oil ratio has an influence on the diffusion behavior of residue oil molecules within the catalyst pores. Because the oil partial pressure is much lower than the hydrogen partial pressure, the effect of H_2/oil ratio is

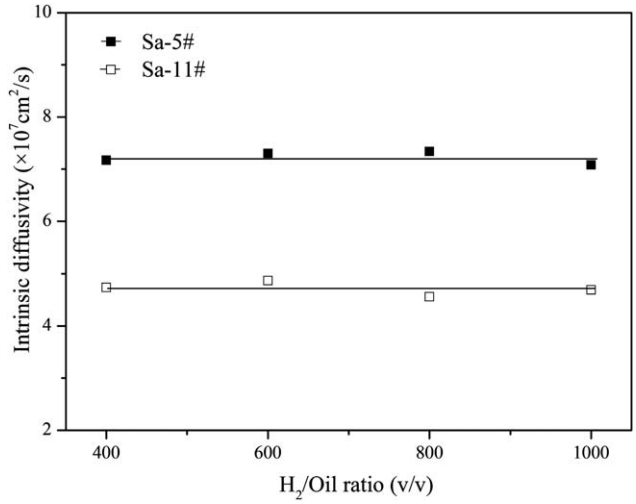

Figure 9. Effect of H_2/Oil (v/v) ratio on intrinsic diffusivity of residue oil cuts (AR-200 catalyst, 385°C, 6.0 MPa).

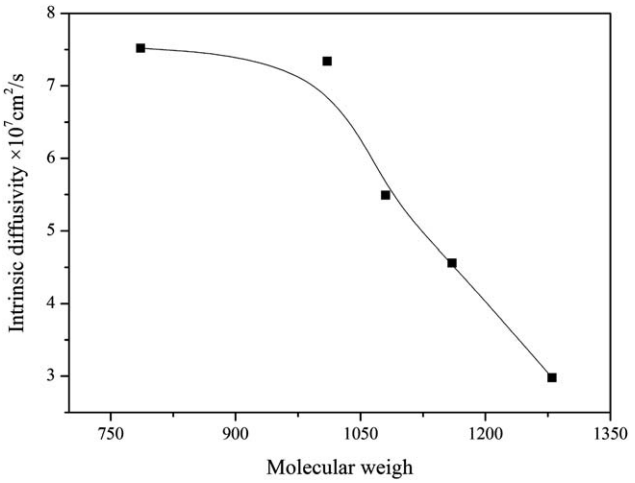

Figure 10. Intrinsic diffusivity of the five narrow cuts (AR-200 catalyst, 400°C, 6.0 MPa, H_2/Oil (v/v) ratio = 800).

expected to mirror the effect of hydrogen pressure. The residue oil was satuated by the H_2 gas, and high H_2/oil ratio can increase the gas-phase fraction in the gas-liquid equilibrium system only, and almost has no influence on the properties (e.g., the viscosity) of liquid phase. As a result, the H_2/Oil ratio has no influence on the diffusion behavior of residue oil molecules.

Intrinsic diffusivity of different narrow cuts

The intrinsic diffusivities of the five narrow fractions shown in Table 1 were measured over AR-200 catalyst and are plotted as a function of molecular weight in Figure 10. Reaction conditions were as follows: 400°C, 6.0 MPa, and H_2/Oil ratio = 800. As discussed in the section of catalyst pore diameter, the internal diffusion in AR-200 catalyst is almost free diffusion, for example, the intrinsic diffusivities in the pores of AR-200 catalyst are almost the bulk diffusivities.

The intrinsic diffusivity decreased with the increase of molecular weight, declining sharply when the molecule weight was larger than 1000. Kyriacou et al.[8] and Liu et al.[12] investigated the diffusivity of different narrow cuts at nonreaction conditions, and they found that the effective diffusivity declined more rapidly, when the molecule weight was higher than 1000. Although the diffusivity obtained at nonreaction conditions is not as valuable as that obtained in hydrotreating reaction conditions, the dependence of diffusivity on the heavy oil molecular weight has general meaning to the heavy oil diffusion. The contents of aromatics and resins in heavy oil increase with molecular weight, and therefore, the polarity and structural complexity of the heavy oil molecules increase and the molecules are more disk-like than rod-like as their molecular weight gets high.[24,25] Deen et al.[46] and Bohrer et al.[47] reported less hindrance to transport of rod-like molecules than disk-like molecules. Therefore, we suppose that the differences in the molecular shape have big impact on the intraparticle diffusion. Differences in molecular structure between the sulfur-containing compounds in heavy and in light fractions may result in different exponents in the Beck–Shultz equation. In addition, the sulfur-containing compounds in the heavy fraction, with higher polarity, could be more strongly adsorbed onto the pore wall than those in the light fraction, as a result, the diffusion rate might be reduced.

Conclusions

The WDUPS catalysts were prepared and used to study the intraparticle diffusion of fractionated Saudi vacuum residue under HDS reaction conditions in a trickle-bed reactor. Credible intrinsic and bulk diffusivities of residue oil molecules were obtained for the first time through measuring the intrinsic and apparent reaction rate constants. The intrinsic diffusivities obtained was found in the range of 2×10^{-7}–8×10^{-7} cm^2/s. The intrinsic diffusivity decreased significantly as the molecular weight of the oil fraction become heavier, and diffusion deviated from bulk diffusivity when the ratio of molecular diameter to pore diameter larger than 0.04. The Beck and Shultz correlation for restrictive diffusion showed that the exponent z was inversely correlated with molecular weight; $z = 3.22$ for the heavy fraction cut and $z = 2.0$ for the light fraction cut. The intrinsic diffusivities increased with the reaction temperature, and did not change significantly with the reaction pressure, or the H_2/Oil ratio.

Acknowledgment

The authors acknowledge the financial support provided by the CNPC (China National Petroleum Corporation) and the National Natural Science Foundation of China (Grant No. 20976192).

Notation

C = bulk concentration of reactant, g/m^3
C_0 = sulfur concentration in feed, g/m^3
C_t = sulfur concentration in product, g/m^3
d_m = molecular average diameter, nm
d_p = average pore size of catalyst, nm
D_i = intrinsic diffusivity in the catalyst pore, cm^2/s
D_e = effective diffusivity in the catalyst pore, cm^2/s
D_b = bulk diffusivity, cm^2/s
$F(\lambda)$ = restrictive factor
k_a = apparent reaction rate constant, m/h
k_i = intrinsic reaction rate constant, m/h
k_n = intrinsic reaction rate constant of reactive order of n
K = Boltzmann constant
M_w = molecular weight
N = reaction order
Q = feedstock flow rate, m^3/h
R = catalyst particle radius, m
S = surface area of catalyst, m^2
S_g = specific surface area of catalyst, m^2/g
SHSV = surface-area hourly space velocity, m^3 oil h^{-1}/m^2 cat
T = absolute temperature of system, K
z = parameter in Eq. 10

Greek Letters

τ = tortuosity of the catalyst
ε = porosity of the catalyst
λ = ratio of molecule size to pore size
ϕ = Thiele modules
η = effectiveness factor
ρ_c = particle density of catalyst, g/m^3
μ = viscosity of solvent, Pa·s

Literature Cited

1. Song C. An overview of new approaches to deep desulfurization for ultra-clean gasoline, diesel fuel and jet fuel. *Catal Today*. 2003;86:211–263.
2. Chen S-L, Dong P, Xu K, Qi Y, Wang D. Large pore heavy oil processing catalysts prepared using colloidal particles as templates. *Catal Today*. 2007;125:143–148.

3. Absi-Halabi M, Stanislaus A, Al-Mughni T, Khan S, Qamra A. Hydroprocessing of vacuum residues: relation between catalyst activity, deactivation and pore size distribution. *Fuel*. 1995;74:1211–1215.
4. Sie ST. Intraparticle diffusion and reaction kinetics as factors in catalyst particle design. *Chem Eng J Biochem Eng J*. 1993;53:1–11.
5. Lee SY, Seader JD, Tsai CH, Massoth FE. Restrictive liquid-phase diffusion and reaction in bidisperse catalysts. *Ind Eng Chem Res*. 1991;30:1683–1693.
6. Pappenheimer JR. Passage of molecules through capillary walls. *Physiol Rev*. 1953;33:387–423.
7. Sane RC, Tsotsis TT, Webster IA, Ravi-Kumar VS. Studies of asphaltene diffusion and structure and their implications for resid upgrading. *Chem Eng Sci*. 1992;47:2683–2688.
8. Kyriacou KC, Sivaramakrishna VV, Baltus RE, Rahimi P. Measurement of diffusion coefficients of oil residual fractions using porous membranes. *Fuel*. 1988;67:15–18.
9. Sane RC, Webster IA, Tsotsis TT. A study of asphaltene diffusion through unimodal porous membranes. *Stud Surf Sci Catal*. 1988;38:705–716.
10. Chen Z, Xu C, Gao J, Zhao S, Xu Z. Hindered diffusion of residue narrow cuts through polycarbonate membranes. *AIChE J*. 2010;56:2030–2038.
11. Liu ZY, Chen SL, Ge XJ, Dong P, Gao JS, Xu ZM. Measurement of diffusion coefficient of heavy oil in fluidized catalytic cracking (FCC) catalysts. *Energy Fuel*. 2010;24:2825–2829.
12. Liu Z, Chen S-L, Dong P, Gao J, Ge X, Xu Z. Diffusion coefficient of petroleum residue fractions in a SiO_2 model catalyst. *Energy Fuel*. 2009;23:2862–2866.
13. Yang X, Guin JA. Diffusion-controlled adsorptive uptake of coal and petroleum asphaltenes in a $NiMo/Al_2O_3$ hydrotreating catalyst. *Chem Eng Commun*. 1998;166:57–79.
14. Wang G, Chen ZT, Lan XY, Wang W, Xu CM, Gao JS. Restricted diffusion of residual molecules in catalyst pores under reactive conditions. *Chem Eng Sci*. 2011;66:1200–1211.
15. Lee SY, Seader JD, Tsai CH, Massoth FE. Restrictive diffusion under catalytic hydroprocessing conditions. *Ind Eng Chem Res*. 1991;30:29–38.
16. Chen Y-W, Tsai M-C, Li C, Kang B-C. Effect of restrictive diffusion on hydrodesulfurization of heavy residue oils over CoMo/Al_2O3. *Can J Chem Eng*. 1994;72:854–861.
17. Li C, Chen Y-W, Tsai M-C. Highly restrictive diffusion under hydrotreating reactions of heavy residue oils. *Ind Eng Chem Res*. 1995;34:898–905.
18. Tsai MC, Chen YW, Li C. Restrictive diffusion under hydrotreating reactions of heavy residue oils in a trickle bed reactor. *Ind Eng Chem Res*. 1993;32:1603–1609.
19. Chen A-C, Chen S-L, Hua D-R, Zhou Z, Wang Z-G, Wu J, Zhang J-H. Diffusion of heavy oil in well-defined and uniform pore-structure catalyst under hydrodemetallization reaction conditions. *Chem Eng J*. 2013;231:420–426.
20. McGreavy C, Draper L, Kam EKT. Methodologies for the design of reactors using structured catalysts: modelling and experimental study of diffusion and reaction in structured catalysts. *Chem Eng Sci*. 1994;49:5413–5425.
21. Philippopoulos C, Papayannakos N. Intraparticle diffusional effects and kinetics of desulfurization reactions and asphaltenes cracking during catalytic hydrotreatment of a residue. *Ind Eng Chem Res*. 1988;27:415–420.
22. Chen J, Yang H, Ring Z. Study of intra-particle diffusion effect on hydrodesulphurization of dibenzothiophenic compounds. *Catal Today*. 2005;109:93–98.
23. Yang CH, Du F, Zheng H, Chung KH. Hydroconversion characteristics and kinetics of residue narrow fractions. *Fuel*. 2005;84:675–684.
24. Shi T-P, Hu Y-X, Xu Z-M, Su T, Wang R-A. Characterizing petroleum vacuum residue by supercritical fluid extraction and fractionation. *Ind Eng Chem Res*. 1997;36:3988–3992.
25. Zhao S, Xu Z, Xu C, Chung KH, Wang R. Systematic characterization of petroleum residua based on SFEF. *Fuel*. 2005;84:635–645.
26. Rudzinski WE, Aminabhavi TM. A review on extraction and identification of crude oil and related products using supercritical fluid technology. *Energy Fuel*. 2000;14:464–475.
27. Chung K, Xu C, Gray M, Zhao Y, Kotlyar L, Sparks BD. The chemistry, reactivity, and processability of athabasca bitumen pitch. *Rev Process Chem Eng*. 1998;1:41–79.
28. Zhou Z, Chen S-L, Hua D, Wang Z-G, Chen A-C, Wang W-H. Tailored ordered porous alumina with well-defined and uniform pore-structure. *Chem Eng J*. 2013;223:670–677.
29. Zhou Z, Chen S-L, Hua D, Chen A-C, Wang Z-G, Zhang J-H, Gao J. Structure and activity of NiMo/alumina hydrodesulfurization model catalyst with ordered opal-like pores. *Catal Commun*. 2012;19:5–9.
30. Zhou Z, Chen S-L, Hua D, Zhang J-H. Preparation and evaluation of a well-ordered mesoporous nickel-molybdenum/silica opal hydrodesulfurization model catalyst. *Transit Metal Chem*. 2012;37:25–30.
31. Comiti J, Renaud M. A new model for determining mean structure parameters of fixed beds from pressure drop measurements: application to beds packed with parallelepipedal particles. *Chem Eng Sci*. 1989;44:1539–1545.
32. Mederos FS, Ancheyta J, Chen JW. Review on criteria to ensure ideal behaviors in trickle-bed reactors. *Appl Catal A*. 2009;355:1–19.
33. Perego C, Peratello S. Experimental methods in catalytic kinetics. *Catal Today*. 1999;52:133–145.
34. Al-Dahhan MH, Duduković MP. Catalyst bed dilution for improving catalyst wetting in laboratory trickle-bed reactors. *AIChE J*. 1996;42:2594–2606.
35. Bej SK. Performance evaluation of hydroprocessing catalysts - a review of experimental techniques. *Energy Fuel*. 2002;16:774–784.
36. Chen J, Ring Z. HDS reactivities of dibenzothiophenic compounds in a LC-finer LGO and H_2S/NH_3 inhibition effect. *Fuel*. 2004;83:305–313.
37. Beck RE, Schultz JS. Hindrance of solute diffusion within membranes as measured with microporous membranes of known pore geometry. *Biochem Biophys Acta Biomembr*. 1972;255:273–303.
38. Renkin EM. Filtration, diffusion, and molecular sieving through porous cellulose membranes. *J Gen Physiol*. 1954;38:225–243.
39. Wilke CR, Chang P. Correlation of diffusion coefficients in dilute solutions. *AIChE J*. 1955;1:264–270.
40. Lee SY, Seader JD, Tsai CH, Massoth FE. Solvent and temperature effects on restrictive diffusion under reaction conditions. *Ind Eng Chem Res*. 1991;30:607–613.
41. Galiasso R, Morales A. Adsorption mechanism of boscan porphyrins on HDM catalysts: III. *Diffusion of porphyrins*. *Appl Catal A*. 1983;7:57–74.
42. Seo G, Massoth FE. Effect of pressure and temperature on restrictive diffusion of solutes in aluminas. *AIChE J*. 1985;31:494–496.
43. Cai H-Y, Shaw J, Chung K. Hydrogen solubility measurements in heavy oil and bitumen cuts. *Fuel*. 2001;80:1055–1063.
44. Prather JW, Ahangar AM, Pitts WS, Henley JP, Tarrer AR, Guin JA. Solubility of hydrogen in creosote oil at high temperatures and pressures. *Ind Eng Chem Process Des Dev*. 1977;16:267–270.
45. So BYC, Klaus EE. Viscosity-pressure correlation of liquids. *ASLE Trans*. 1980;23:409–421.
46. Deen WM, Bohrer MP, Epstein NB. Effects of molecular size and configuration on diffusion in microporous membranes. *AIChE J*. 1981;27:952–959.
47. Bohrer MP, Fetters LJ, Grizzuti N, Pearson DS, Tirrell MV. Restricted diffusion of linear and star-branched polyisoprenes in porous membranes. *Macromolecules*. 1987;20:1827–1833.

Manuscript received July 24, 2013, and revision received May 7, 2014.